SLAC-PUB-10486
June 2004

Simulation of Dark Currents in X-band Accelerator Structures *

K.L.F. Bane, V.A. Dolgashev, G.V. Stupakov,
Stanford Linear Accelerator Center, Stanford University,
Stanford, CA 94309 USA

Presented at the Ninth European Particle Accelerator Conference (EPAC'04),
Lucerne, Switzerland
July 5-9, 2004

*Work supported by Department of Energy contract DE–AC03–76SF00515.

SIMULATION OF DARK CURRENTS IN X-BAND ACCELERATOR STRUCTURES*

K.L.F. Bane, V.A. Dolgashev, G.V. Stupakov, SLAC, Menlo Park, CA 94025, USA

INTRODUCTION

In high gradient accelerator structures, such as are used in the main linac of the Next Linear Collider (NLC) [1], electrons are emitted spontaneously from structure walls and then move under the influence of rf fields. A question of interest for the NLC is, what is the effect of such "dark current" electrons on the main linac bunch, *e.g.* can they significantly affect its orbit or emittance? To help answer this question we have taken a dark current simulation program and modified it to estimate such effects (see Ref. [2]).

In this report we use the dark current program—a Mathematica program written by S. Setzer [3]—to study properties of dark currents themselves. Dark currents have been studied by many authors, both experimentally and through numerical tracking (see *e.g.* Refs. [3]–[6]). A difference from earlier numerical work is that, instead of choosing many random positions and times of emission, we consider all possible emissions (with some resolution) from the irises of a structure. We address questions such as: what fraction of dark current reaches the ends of a structure, what are the temporal and spectral distributions of outgoing dark current, and what is the gradient dependence. Our calculations do not include the generation of secondary electrons (we believe they are not important in their effect on a bunch). This is thus a study of the behavior of *primary* dark current electrons in X-band accelerator structures. Note however that, in a real structure, primary electrons may be outnumbered by secondary electrons (as was found, for example, in a high gradient S-band study [5]). More details of our results will be given in a future report.

SIMULATION PROGRAM

S. Setzer's program can handle periodic structures of any length. For travelling wave structures, first MAFIA [7] is used to obtain electric and magnetic fields (complex quantities) over a fine grid that covers one cell. This data is splined to give the fields as functions of radial and longitudinal coordinates (r, z). The Floquet condition then gives the fields in any cell of a repeating structure. Finally, time dependence is added by multiplying (with the proper phase) with $e^{i\omega t}$, where ω is the rf frequency and t is time.

The structure that we consider in this report is the H60VG3 disk-loaded structure, a 54-cell, approximately constant gradient cavity that was built for the NLC project, and that operates at 11.4 GHz with a per cell phase advance of 150°. For our calculations we take a model with identical cells, with dimensions of the average H60VG3 cell: iris radius $a = 4.7$ mm, cavity radius $b = 11.1$ mm, gap $g = 6.9$ mm, and period $p = 10.9$ mm (see Fig. 1). We set the field strengths so that the locally averaged, on-axis gradient, is everywhere $E_{acc} = 65$ MV/m.

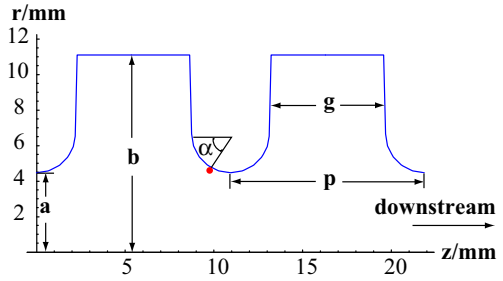

Figure 1: Two cells of the model geometry, showing the angle α (the emission point is given by the red dot).

For dark current simulations consider now an iris emission point at angle α, defined with respect to the upstream horizontal (see Fig. 1). We allow charged macro-particles, initially at rest, to be pulled away from the walls by the rf fields. We let the time development of the charge of emitted particles to follow the Fowler-Nordheim (F-N) equation [8]

$$J = 1.54\times 10^{-6}\frac{\beta^2 E^2}{\varphi}10^{4.52\varphi^{-0.5}}\exp\left[-\frac{6.53\times 10^9\varphi^{1.5}}{\beta E}\right] \quad (1)$$

with J the current density (in A/m^2), β the field enhancement factor, φ the work function of the metal (in eV), and E the applied electric field (in V/m). In our simulations we take $\varphi = 4.7$ eV (copper) and $\beta = 30$. Note that in this report we consider relative currents only, and the size of emitters is not important. After particles leave the wall they are tracked until they either hit a wall or leave the structure.

In Fig. 2 we plot example dark current trajectories, in normalized time steps $\Delta\theta \equiv (180/\pi)\,\omega\Delta t = 1^\circ$, for emission angles $\alpha = 65^\circ$, 90°, and 115°. Only trajectories with current densities within 1% of the maximum are shown; they are color coded to give current density (maximum is blue, small is red) or, equivalently, time of emission. Black dots give snapshots of macro-particle positions, beginning when the last particle has been emitted and then in $c\Delta t = 1$ cm steps (c is speed of light). We see that in all 3 cases most particles end up colliding with the opposite iris/cell. Example 1 has significant "capture," by which we mean particles that get caught by the rf wave and travel long distances through the structure. We see that the captured particles were emitted later in time than peak emission, and they end up filling almost the entire aperture. Example 3 shows significant upstream drift. The drifting particles were emitted earlier in time than peak emission, and the drift distance is limited to a half dozen or so cells.

*Work supported by the Department of Energy, contract DE-AC03-76SF00515

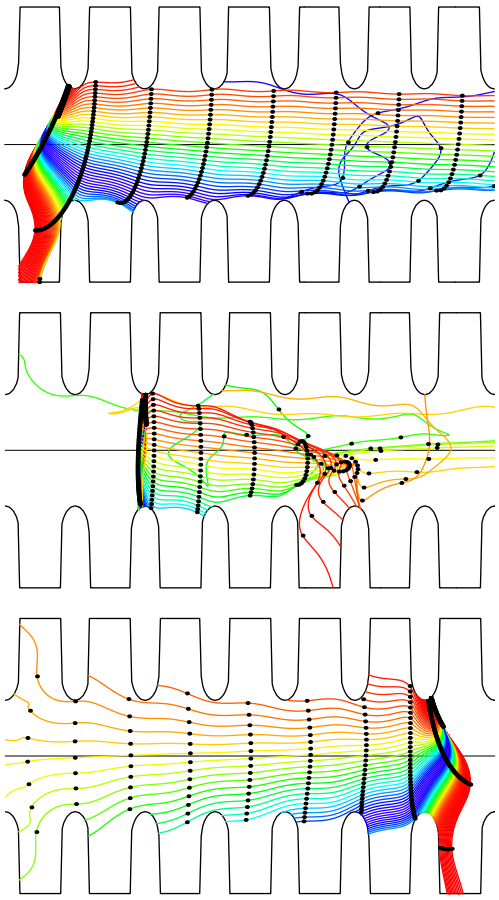

Figure 2: Dark current traces for emission angles $\alpha = 65°$ (top frame), $90°$ (middle), and $115°$ (bottom). Particles are emitted from above. Downstream is to the right.

To study capture we calculate the fraction of emitted current that reaches 54 cells downstream, I_{dn}, as function of α, in $2.5°$ steps (see Fig. 3). Here the emission time step is $\Delta\theta = 0.1°$. We note that capture is maximized when emission is from the upstream end of an iris, at angle $63°$.

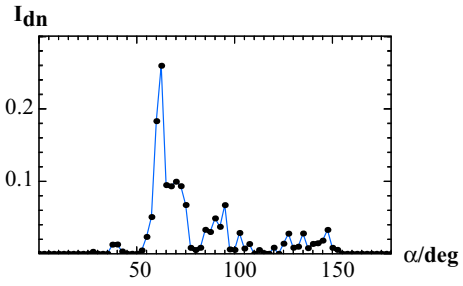

Figure 3: Fraction of emitted current that reaches 54 cells downstream *vs.* α.

OUTGOING CURRENT

Let us study the outgoing current (both up- and downstream) from a 54-cell structure. We assume that there are many emitters, so that we can average over trajectories. We take each iris to have emitters (of equal size) all around the tip, and all irises to emit equally. For the calculations we take a 108-cell, periodic model that emits from the middle iris, and save macro-particle properties at cell boundaries. From these results, by making assumptions about the α dependence of emitted current and performing sums, we obtain properties of the outgoing current in a 54-cell cavity. Note that in experiment at SLAC a cavity is connected at both ends to 20 cm of vacuum chamber and then to detectors (beam current monitors). In our simulations, to estimate the current that reaches the detectors, we finally collimate out all outgoing particles with angles large enough to impinge on 20 cm tubes of radius a.

The α dependence of emitted current is not known. We will, therefore, take two very different assumptions and compare results, with the idea of obtaining a range over which the real answer is likely to lie. The first assumption, which we call the *non-uniform* assumption, is that the F-N equation, with the same β, also applies at different iris positions. The maximum electric field on the iris surface varies from 85 MV/m at $\alpha = 90°$, to 130 MV/m at $\alpha = 25°$, $155°$. Under the non-uniform assumption the importance of emission angles near $25°$, $155°$, will be strongly enhanced. However, this assumption does not seem to agree with observation; *e.g.* pitting on iris surfaces, which is thought to be indicative of dark current emission [11], is not preferentially found at angles of maximum field. We take as second assumption, the *uniform* assumption, under which the peak current density is independent of α. Note that even if the F-N equation is thought to be applicable microscopically, if the local β values vary randomly by a number large compared to 40%, the uniform assumption may be more pertinent.

In our simulations the emission time step is $\Delta\theta = 0.1°$; the emission angle α ranges over $[0°, 180°]$ in $5°$ steps. Fig. 4i gives, for the uniform assumption, the fraction of emitted current I that exits the structure (solid) and reaches the detectors (dashes), as functions of cell of origination, n_{cell}. We see from the relatively flat region of the downstream curves that many particles are captured. The large difference between both pairs of curves at the ends indicates that many particles generated near the ends have large angles and are collimated away. Fig. 4ii gives the running sum accumulated from the ends of the cavity, I_{run}. We see that for the uniform (non-uniform) assumption 2.2% (0.3%) of emitted current reaches the downstream detector; for the upstream detector the results are 0.1% (0.05%). Note that a typical *measured* ratio of upstream to downstream current in NLC structures is a factor of 10 [9].

Fig. 5 displays, for emission uniform in α, the time distributions (normalized to emitted current) of the outgoing current at the ends of the structure and at the detectors. We see that the downstream current is well bunched (for capture $0 \leq ct \leq \lambda/4$), whereas the upstream current is not. Note that the upstream current is mostly collimated away before reaching the detector. In Fig. 6 we display the distribution of the downstream kinetic energy $\mathcal{E}_k$, again for the uniform assumption. We can see that it is the low en-

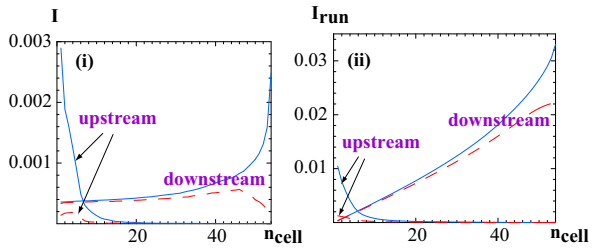

Figure 4: For emission uniform with α: (i) Fraction of emitted dark current exiting the structure (solid) and reaching the detectors (dashes) as functions of cell of origination n_{cell}. Frame (ii) gives the running sum accumulated from the ends of the structure.

ergy particles that have large angles, and are therefore collimated away. Note that the maximum energy is 28 MeV, whereas $E_{acc}L = 38$ MV (L is structure length). The upstream distributions (not shown) are rather uniform and limited to $\mathcal{E}_k < 2$ MeV.

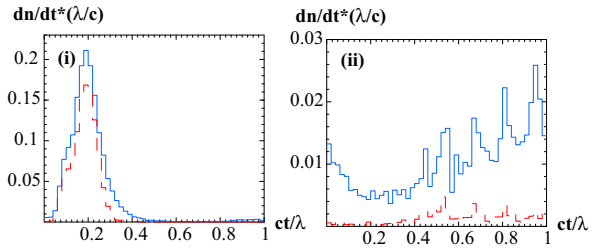

Figure 5: Time distribution of dark current exiting the structure (solid) and entering the detectors (dashes), at the upstream (i) and downstream (ii) ends.

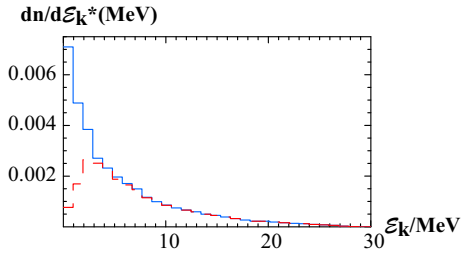

Figure 6: Distribution in kinetic energy of dark current exiting the structure (solid) and entering the detectors (dashes), at the downstream end.

GRADIENT DEPENDENCE

We have repeated the simulations for different gradients. In Fig. 7 we give the gradient dependence of the fraction of emitted current reaching the downstream (i), and upstream (ii) detectors, when assuming uniform (solid line) and non-uniform (dashes) emission. We note that capture rises steeply near $E_{acc} = 50$ MV/m. Note that this is less than the gradient necessary to capture a particle from rest, $E_{acc} = \pi m_0 c^2/\lambda = 61$ MV/m [10]. Finally, in Fig. 8 we plot the downstream data as $1/E_{acc}$ *vs.* $\ln(\mathcal{I}_{dn}/E_{acc}^{2.5})$ ($\mathcal{I}_{dn}$ is outgoing dark current, in arbitrary units). Measured dark current is often plotted this way, fitted to a straight line, and the slope is used to give a β to characterize a structure [11]. Our fitted slopes are 13% steeper than the emitted current curve. Such a measurement procedure will, therefore, overestimate the effective β within a structure by 13%.

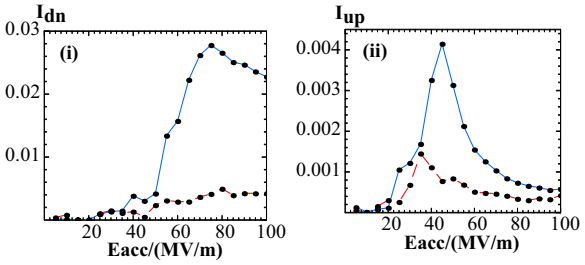

Figure 7: Gradient dependence of fraction of emitted current reaching downstream (i) and upstream (ii) detectors, for uniform (solid line), non-uniform (dashes) emission.

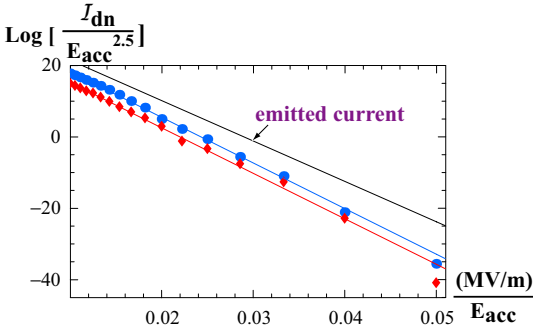

Figure 8: Fowler-Nordheim plot of dark current reaching downstream detector, assuming uniform (circles) or non-uniform (diamonds) emission. Lines give linear fits and the emitted current.

ACKNOWLEDGEMENTS

The authors thank S. Setzer for providing us with his computer program, Juhao Wu for help in modifying the code, and C. Adolphsen and R. Miller for helpful comments and suggestions.

REFERENCES

[1] "NLC Design Report," SLAC Report 474, 1996.
[2] V. Dolgashev, *et al*, paper WEPLT155, this conference.
[3] S. Setzer, *et al*, Proc. PAC03, 3566 (2003).
[4] J. Wang, G. Loew, *IEEE Trans. Nucl. Sci.* **32**, 2915 (1985).
[5] S. Yamaguchi, LAL/RT 92-18, Orsay, Dec. 1992.
[6] V. Ivanov, *et al*, Proc. PAC03, 2664 (2003).
[7] "MAFIA User Manual," CST GmbH, Darmstadt, Germany.
[8] R. Fowler, L. Nordheim, *Proc. Roy. Soc* **A119**, 173 (1928).
[9] C. Adolphsen, private communication.
[10] R. Helm, R. Miller, in P. Lapostolle and A. Septier (eds.), *Linear Accelerators*, (North-Holland, Amsterdam, 1970).
[11] J. Wang, PhD thesis, SLAC Report 339, 1989.